

## Proximity dc squids in the long-junction limit

L. Angers, F. Chiodi, G. Montambaux, M. Ferrier, S. Guéron, and H. Bouchiat  
*Laboratoire de Physique des Solides, Université Paris-Sud, CNRS, UMR 8502, F-91405 Orsay Cedex, France*

J. C. Cuevas

*Departamento de Física Teórica de la Materia Condensada, Universidad Autónoma de Madrid, 28049 Madrid, Spain*

(Received 31 July 2007; revised manuscript received 29 January 2008; published 7 April 2008)

We report the design and measurement of superconducting/normal/superconducting (SNS) proximity dc squids in the long-junction limit, i.e., superconducting loops interrupted by two normal metal wires, which are roughly a micrometer long. Thanks to the clean interface between the metals, a large supercurrent flows through the device at low temperature. The dc squidlike geometry leads to an almost complete periodic modulation of the critical current through the device by a magnetic flux, with a flux periodicity of a flux quantum  $h/2e$  through the SNS loop. In addition, we examine the entire field dependence, notably the low and high field dependences of the maximum switching current. In contrast to the well-known Fraunhofer-type oscillations typical of wide junctions, we find a monotonous Gaussian extinction of the critical current at high field. As shown by Cuevas and co-workers [Phys. Rev. B **76**, 064514 (2007); Phys. Rev. Lett. **99**, 217002 (2007)], this monotonous dependence is typical of long and narrow diffusive junctions. We also find in some cases a puzzling reentrance at low field. In contrast, the temperature dependence of the critical current is well described by the proximity effect theory, as found by Dubos *et al.* [Phys. Rev. B **63**, 064502 (2001); Phys. Rev. Lett. **87**, 206801 (2001)] on SNS wires in the long-junction limit. The switching current distributions and hysteretic  $IV$  curves also suggest interesting dynamics of long SNS junctions with an important role played by the diffusion time across the junction.

DOI: [10.1103/PhysRevB.77.165408](https://doi.org/10.1103/PhysRevB.77.165408)

PACS number(s): 74.45.+c

### I. INTRODUCTION

The proximity effect, or the penetration of superconducting correlations in a normal (nonsuperconducting) conductor due to the proximity to a superconducting one, has been shown to give normal conductor superconductinglike properties over a length that can be considerable at low temperatures. This happens when the phase coherence length extends beyond the length of the normal metal and when thermal fluctuations are small enough. This quantum coherence of a mesoscopic conductor then ensures that Andreev pairs, which are pairs of time-reversed electrons, can propagate over distances of the order of the phase coherence length in the normal metal. Such a length is notably greater than the superconducting coherence length  $\xi_S^N = \sqrt{\hbar D_N / \Delta}$ , where  $\Delta$  is the superconducting gap and  $D_N$  is the diffusion constant in the normal metal. The normal conductors have ranged from simple noble metals to semiconducting planes or wires, to long or short molecules (carbon nanotubes, endohedral fullerenes, and DNA), down to individual atoms in break junction geometries.<sup>1-4</sup>

One of the most remarkable consequences of the proximity effect is the propensity of a normal conductor well connected to two superconductors with different phases to carry a supercurrent, thereby demonstrating that Andreev pairs carry superconducting correlations along with information about the macroscopic phase of the superconductor at the boundary. Depending on the length of the normal part, the maximal supercurrent (called critical current  $I_c$ ) that can be carried is determined either by the superconducting gap of the superconductor or by the characteristic energy of the normal metal, i.e., the so-called Thouless energy, which is given

by  $E_{Th} = \hbar D_N / L_N^2$  in a diffusive conductor. Indeed, the critical current at zero temperature has been shown<sup>5</sup> to be given by  $eR_N I_c(T=0) = 2.07\Delta$  in the case of short junctions ( $L_N < \xi_S^N$ , or equivalently,  $E_{Th} > \Delta$ ) and  $eR_N I_c(T=0) = 10.82E_{Th}$  in the opposite limit of long junctions. More generally, the remarkable point is that in the short-junction limit, the superconductor determines the properties of the proximity system, and in the long-junction limit, it is the normal metal (via its length, diffusion time, and coherence length) that determines the proximity effect.

The interplay of the mesoscopic phase coherence in the normal metal and the superconducting coherence due to the nature of the superconducting state has led to the fabrication of many interferometer devices. The experiments that launched the development of the mesoscopic proximity effect mainly consisted of a normal metal loop, with nearby superconducting islands.<sup>6,7</sup> The resistance of these devices was modulated by the magnetic field 1 or 2 orders of magnitude more than the universal conductance fluctuations in normal rings with no superconductor. However, no supercurrent was measured because normal leads connected the mesoscopic devices. Interferometers in which a supercurrent was obtained and modulated are much more recent and, in most cases, do not use a noble metal as the normal part: the nonsuperconducting part actually is made of a long molecule such as carbon nanotubes<sup>3</sup> or semiconducting wires.<sup>4</sup> In some cases,  $\pi$  junctions can be produced, either by the use of a ferromagnet between superconductors or by the action of a gate electrode, which modulates the population of the normal part.

Interestingly, although many mesoscopic interferometers have been devised with a normal metal between several superconductors,<sup>6,7</sup> no basic plain dc squid interferometer

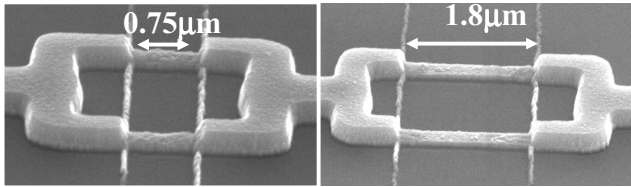


FIG. 1. SEM images of the two Nb/Au/Nb SNS dc squids Nb750 and Nb1200. Insufficient etching of the Nb in the central part of the longest SNS squid (right image) causes the normal region to have a length of 1200 nm instead of 1800 nm.

has yet been devised in the mesoscopic regime.<sup>8,9</sup> In this paper, we describe several proximity dc squids, i.e., superconducting loops with two normal metal bridges, ranging from 0.75 to 1.9  $\mu\text{m}$  long. We find that the  $IV$  curves are hysteretic, which is a phenomenon that we attempt to explain by the intrinsic dynamics of the diffusive normal metal. We find that the temperature dependence of the critical current of each long junction is in accordance with the theory of the proximity effect, much like in the work of Dubos *et al.*<sup>10</sup> The field dependence is more original: In the proximity dc squid configuration, the critical current is highly modulated by the magnetic field. In both the single superconducting/normal/superconducting (SNS) junction and the dc squid configuration at large perpendicular magnetic field, the extinction of the critical current with the field is monotonous and does not show the interference pattern previously observed in wider junctions.<sup>11–13</sup> We present two theoretical models, which attempt to explain this behavior by including the diffusive nature of the normal metal. Finally, a surprising reentrance of the critical current at low field is also observed in some samples and remains unexplained.

The paper is arranged as follows: We first outline the sample fabrication. Then, we describe the transition to the fully developed proximity regime. We next present the current-voltage curves at low and high temperatures and the distribution of switching currents, and then discuss the dynamics of the SNS junctions. The temperature dependence of the switching current follows. Then, we concentrate on the magnetic field dependence of the switching current: We detail the interference pattern in SNS dc squids at low fields; the large scale monotonous field dependence for all samples is then addressed and compared to theoretical predictions. Finally, we report a surprising reentrance for some of the Al based samples.

## II. SAMPLE FABRICATION AND MEASUREMENT APPARATUS

As a normal metal, we used 99.9999% pure gold, with a content in magnetic impurities (Fe) smaller than 0.1 ppm. Weak localization measurements in a simple wire made of this same material (at a different time) determined a phase coherence length of the order of 10  $\mu\text{m}$  below 50 mK.<sup>14</sup> Two different superconductors were used, either aluminum or niobium (see Figs. 1 and 2). The proximity wires and dc squids made from Al and Au were obtained by conventional

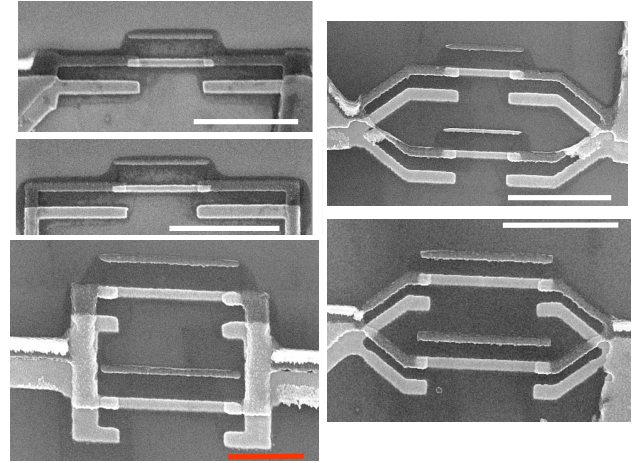


FIG. 2. (Color online) SEM pictures of Al/Au/Al SNS wires and SNS dc squids. From top to bottom wires Alw1250 and Alw1300 and from left to right: SNS dc squids Alsq1500, Alsq900, and Alsq1900. The scale bar is 2  $\mu\text{m}$ .

double angle thermal evaporation through a suspended mask in a vacuum of  $10^{-6}$  mbar. The process with niobium as a superconductor is more involved. We start with a bilayer of 50 nm thick thermally evaporated gold, which is covered by a 200 nm thick layer of sputtered niobium, and cover the bilayer with a 70 nm thick aluminum layer. With  $e$ -beam lithography, we define and wet-etch open a window in the Al mask through which we locally etch away the Nb using an SF<sub>6</sub> plasma. In a realignment step, we create a ring or wire shaped Al mask around which the bilayer is removed by an SF<sub>6</sub> reactive ion etch followed by an argon ion beam etch. Finally, the Al mask is removed and the samples are tested before cooling down. The sample parameters, obtained via scanning electron microscopy (SEM) visualization or transport measurements, are gathered in Table I.

The length of the normal metal, which varies between 0.75 and 1.9  $\mu\text{m}$ , is much greater than the superconducting coherence length,  $\xi_S^N = \sqrt{\hbar D_N / \Delta}$ , where  $\Delta$  is the BCS superconducting energy gap (see the ratio  $\Delta / E_{Th}$  in Table I). Thus, the devices are in the long-junction regime, in which the properties of the normal metal are known to determine the proximity effect, rather than the properties of the superconductor.<sup>15</sup>

The two superconductors used, i.e., Nb and Al, differ by their transition temperature. The fabrication procedure also produces different S/N interface conditions: In the Nb/Au samples, the superconductor is a homogeneous bilayer of Nb/Au and the normal metal is a bare Au region. In contrast, in the angle-evaporated samples of Al/Au, the bare Au wires contact a region where Au and Al overlap (see the SEM image). In addition, the Al loop is, at some point (depending on the loop shape, see image), covered by Au. Therefore, the superconductor in this configuration is less homogeneous.

The geometry of the SNS long junction is similar to previously measured ones.<sup>10,16</sup> To our knowledge, the simple SNS dc squid geometry has not yet been reported in mesoscopic samples. An SNS dc squid with submillimeter-wide

TABLE I. Characteristics of the different samples.  $L_N$  and  $W$  are, respectively, the length and width of the normal metal, which was 50 nm thick high purity (99.9999%) gold for all samples.  $E_{Th} = \hbar D_N / L_N^2$  is the Thouless energy, with  $D_N$  as the diffusion constant in the normal metal. Note that  $\xi_S^N = \sqrt{\hbar D_N} / \Delta$  is the superconducting coherence length determined from the gap of the superconductor, but using the diffusion constant in the normal wire, so that it is evaluated via  $\xi_S^N = L_N \sqrt{E_{Th}} / \Delta$ . The Al SNS wires (labeled Alwx, with  $x$  as the length of the normal wire in nanometers) were all produced on the same chip and therefore should have the same material constants. This is also true for the Al SNS dc squids (labeled Alsqx) and for the Nb SNS dc squids (labeled Nbx). The superconducting gap  $\Delta$  is deduced from the transition temperature of the superconducting contacts using  $\Delta / k_B = 1.76 T_c$ .  $I_s^{\max}$  and  $I_s^{\min}$  are, respectively, the maximal and minimal switching currents measured at the lowest temperature and correspond, respectively, to constructive ( $\Phi / \Phi_0 = n$ ) and destructive ( $\Phi / \Phi_0 = n + 1/2$ ) interferences in the dc squids.  $I_r$  is the retrapping current (see text).  $T^*$  marks the transition temperature from classical to quantum (see text).

	Nb750	Nb1200	Alw900	Alw1300	Alw1250	Alsq900	Alsq1500	Alsq1900
Geometry	SNS dc squid	SNS dc squid	SNS wire	SNS wire	SNS wire	SNS dc squid	SNS dc squid	SNS dc squid
$L_N$ ( $\mu\text{m}$ )	0.75	1.2	0.9	1.3	1.25	0.9	1.5	1.9
$W$ ( $\mu\text{m}$ )	0.4	0.4	0.125	0.125	0.125	0.13	0.15	0.2
$\Delta / k_B$ (K)	16	16	2.8	2.8	2.8	2.8	2.8	2.8
$E_{Th}$ from high $T$ fit (mK)	140	50	33	36	44	47	30	26
$\Delta / E_{Th}$	114	320	85	78	64	60	93	108
$\xi_S^N = L_N \sqrt{E_{Th}} / \Delta$ (nm)	70	67	100	150	156	116	155	180
$R_N$ from $dV/dI$ ( $\Omega$ )	0.4	0.7	5	5	6	2.6	3.3	3
$I_s^{\max}$ ( $\mu\text{A}$ )	330	68	13	3.7	4.3	17	7.6	4.6
$I_s^{\min}$ ( $\mu\text{A}$ )	170	26				9.2	1.8	0.6
$I_r$ ( $\mu\text{A}$ )	75	16	1	0.6	0.6	1.3	1	0.45
$b = e R_N I_s^{\max} / E_{Th}$	11	11	22	6	7	11	10	6
$I_s / I_r$	4.4	4.25	13	6.2	7.2	13	7.6	10.2
$\sqrt{2b}$	4.7	4.7	6.6	3.5	3.8	4.7	4.5	3.5
$T^*$ (mK)	100	40	35	20	25	35	21	14

junctions was, however, produced by Clarke and Paterson in 1971 (Ref. 9) in the aim of realizing an amplifier via a tuning of the dc squid asymmetry. This will be detailed further in this paper. Moreover, a more complex SNS dc squid with an adjustable nonequilibrium population of the normal part was realized by Baselmans *et al.*<sup>8</sup> The simplest SNS dc squid consists of a superconducting loop interrupted by two normal metal wires. In our setup, superconducting leads in a four wire configuration connect the loop. In comparison, the usual dc squid is formed by a superconducting loop interrupted by insulating tunnel barriers. A dc supercurrent flows through such a dc squid, and its maximum value, i.e., the switching current, is known to be periodically modulated by a magnetic field, with a period of one flux quantum  $\Phi_0 = h/2e$  through the loop area.

The measurements were conducted via room temperature  $\pi$  filters, homemade cryogenic lossy coaxial cables leading to the dilution stage, and 150 pF parallel capacitors on the sample holder. The samples were current biased with a dc current of up to 400  $\mu\text{A}$  and a small ac current (a few ten to hundred nanoamperes) at a few hundred hertz for differential resistance measurements.

### III. TRANSITION TEMPERATURES

The resistance of two Au/Nb dc squids is plotted in Fig. 3 as they are cooled to low temperature. The first resistance

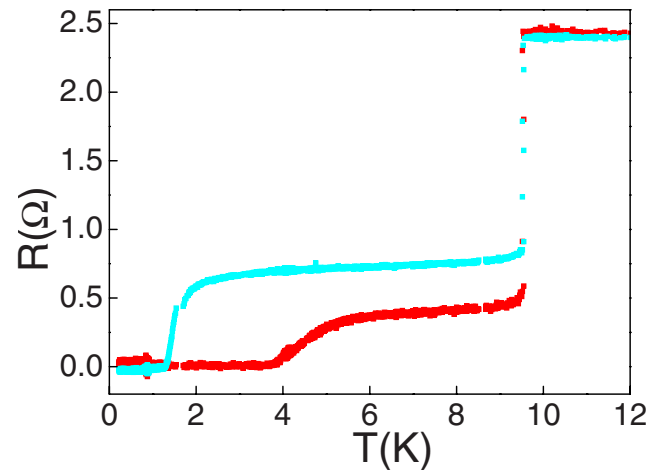


FIG. 3. (Color online) Resistance of the two Nb/Au/Nb proximity dc squids versus temperature during cool down with no applied magnetic field. The configuration is a four-wire measurement. The first transition around 9 K is the superconducting transition of niobium. The transition at the lower temperature (around 5 K for the shortest wire and 2 K for the longest one) is the transition of the gold wire from normal to a proximity-induced superconducting state. Temperatures are only approximate above 4 K due to poor calibration of the thermometer in this range.

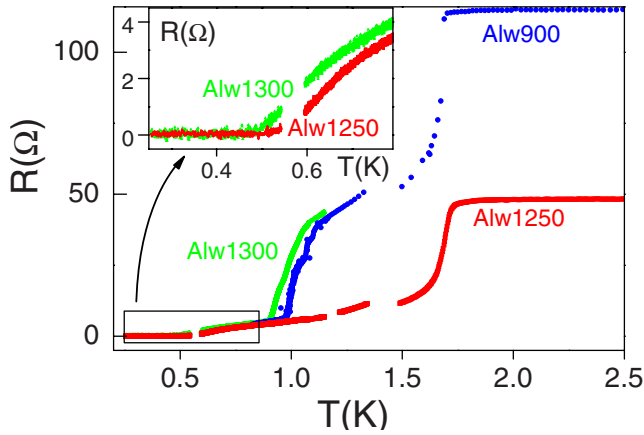


FIG. 4. (Color online) Resistance of three Al/Au/Al wires as a function of the temperature during cool down with no applied magnetic field. Sample Alw1250 is measured in a four-wire configuration, Alw1300 and Alw900 were measured in a three-wire configuration, and constant resistances of 79 and 72  $\Omega$ , respectively, corresponding to the resistance of one lead, have been subtracted. The double transition at 1.6 and 1 K for samples Alw900 and Alw1300 is due to their geometry, in which part of the superconducting wire is made of pure Al with a critical temperature of 1.6 K and part is made of an Al/Au bilayer with a critical temperature of 1 K. Inset: Zoom of the transition to the zero-resistance state of Alw1250 and Alw1300.

drop corresponds to the transition to a superconducting state of the Nb/Au bilayer around 9.5 K. Below the transition temperature, the resistance varies by less than 10% over a large temperature range. The final resistance drop to a zero resistance state occurs at a lower temperature. This temperature corresponds to the temperature below which the supercurrent through the normal wire is measurable. The wire should therefore be phase coherent, and thermal fluctuations should be sufficiently small. This is realized when the temperature is smaller than the Josephson energy of the junction  $E_J(T) = (\hbar/2e)I_c(T)$ .<sup>17</sup> Then, the supercurrent decays roughly as  $e^{-T/(10E_{Th})}$  (see corresponding section). We find that the final resistance drop occurs at temperatures between  $20E_{Th}$  and  $40E_{Th}$  depending on the samples.

The behavior of the three Al/Au SNS wires, which are plotted in Fig. 4, is similar.

#### IV. IV CURVES AND DIFFERENTIAL RESISTANCE

##### A. Experimental curves at low temperature

Typical  $V(I)$  curves are shown in Fig. 5 for an SNS dc squid at two magnetic fields, one in which the interference between both branches is constructive ( $\Phi/\Phi_0 = n$ ) and the other in which the interference is destructive ( $\Phi/\Phi_0 = n + 1/2$ ), with  $n$  as an integer. Single SNS junctions in the long limit have similar  $IV$  curves (not shown). As the current is increased, a supercurrent flows (zero voltage drop) up to a value called the switching current (denoted as  $I_s$ ), above which a voltage drop appears, and the junction is said to have switched to the resistive branch. As the current is de-

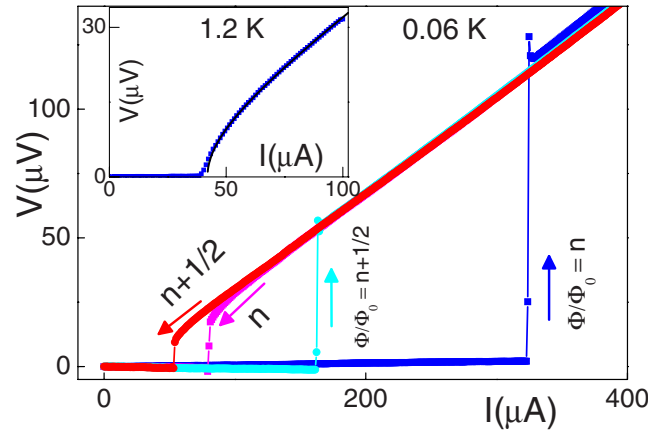


FIG. 5. (Color online) Typical  $V(I)$  curves of SNS dc squids at two magnetic fields, one in which the interference between both branches is constructive ( $\Phi/\Phi_0 = n$ ) and the other in which the interference is destructive ( $\Phi/\Phi_0 = n + 1/2$ ), showing maximum and minimum switching currents. In both cases, the hysteresis is clearly visible and characterized by a large ratio (roughly 3) between switching current  $I_s$  and retrapping current  $I_r$ . The sample measured here is the shortest Au/Nb dc squid Nbsq750. The  $V(I)$  curves for the SNS wires are similar. Inset:  $IV$  curve of the same sample at 1.2 K, where there is no hysteresis. The shape of the curve corresponds to the square-root dependence expected in the overdamped regime, i.e.,  $Q < 1$  (continuous line).

creased, the switch from the resistive branch to the superconducting one occurs at a current called the retrapping current (denoted as  $I_r$ ), which is much smaller than the switching current: The  $IV$  curves are strongly hysteretic, as found in previous experiments.<sup>10,16,18</sup> The value of the retrapping current does not depend on how far we sweep the dc current; nor does it depend on the temperature (for low enough temperatures, see Fig. 8), in stark contrast with the switching current, as described in the next section.

Equivalently, the differential resistance as a function of the dc current is shown in Fig. 6 for an SNS dc squid. The

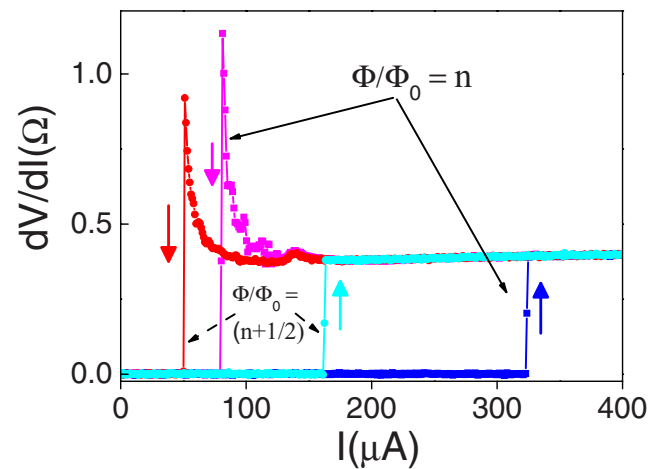


FIG. 6. (Color online) Differential resistance of the shortest Au/Nb dc squid (Nbsq750) at maximum and minimum switching currents at 60 mK.

resistance in the normal state (i.e., when the current through the wire is larger than the critical current) varies with the current by a few percent in the Nb samples and much more in the Al samples probably because of inhomogeneities in the Al and Al/Au superconducting leads, which can generate phase slips. Some features on the down curve before retrapping (strongly fluctuating differential resistance just before retrapping and resistance bump at 140  $\mu\text{A}$ ) are still not fully understood but should be explained by the dynamics of an SNS junction out of equilibrium.<sup>10,19</sup>

In the following paragraphs, we address the questions of the value of the switching current, which is 10%–20% smaller than the critical current of the junction, the degree of hysteresis in the  $IV$  curves, and the fluctuation in the switching current for a given junction, field, and temperature.

## B. Dynamics of the superconducting/normal/superconducting junction: The RSJ model adapted to superconducting/normal/superconducting junctions

### 1. Hysteretic $IV$ curves in superconducting/normal/superconducting junctions

The  $IV$  curves are well understood in superconductor/insulator/superconductor (SIS) tunnel junctions, which are modeled by a Josephson element in parallel with a capacitance and a resistive element [the so-called resistively shunted junction (RSJ) model; see, for instance, Ref. 20]. The elements of the circuit lead to a dynamical equation for the superconducting phase of the junction  $\varphi$  given by

$$\ddot{\varphi} + \frac{1}{\tau_R} \dot{\varphi} + \omega_p^2 \left[ \sin(\varphi) - \frac{I}{I_c} \right] = 0. \quad (1)$$

Here,  $\omega_p = 1/\sqrt{L_K C}$ , where  $L_K$  is the kinetic inductance given by  $L_K = \phi_0/2\pi I_c$  and  $\tau_R = RC$  controls the charge relaxation through the junction. The state of the junction is represented by a particle whose position is the phase evolving in a tilted oscillating potential  $U(\varphi) = -E_J(\cos \varphi + I/I_c \varphi)$ . The slope is the biasing current and the height of the barrier is related to the Josephson energy  $E_J = [\hbar/(2e)]I_c$ . The time scale  $\tau_R = RC$  represents friction for the particle. In the nonresistive state, the particle is trapped in a local minimum and oscillates at the plasma frequency  $\omega_p/2\pi$ . Increasing the current increases the slope of the potential and decreases the barrier height. Eventually, the particle escapes at  $I_s \leq I_c$ . The hysteresis is understood within this model. At high dc bias, the ac Josephson current oscillating at the Josephson frequency  $\omega_J = \hbar/2$  eV flows entirely through the capacitance and does not affect the  $IV$  curve, which is determined by the resistance and is linear. At lower voltage corresponding to  $\omega_J \approx \omega_p$ , there is a nonlinear contribution of the ac to the  $IV$  curve, which increases with decreasing bias. This gives rise to a negative contribution to the differential conductance, leading to hysteretic current biased  $V(I)$  curves.<sup>21</sup> This reasoning leads to  $I_s/I_r \approx RC\omega_p = Q$  and explains why the retrapping current can be much smaller than the switching current if  $\tau_R \gg 1/\omega_p$  or  $Q \gg 1$ .

### 2. Damping and hysteretic $IV$ curves in superconducting/normal/superconducting junctions

However, this model is not directly applicable to the experiments on SNS junctions. The  $\sin(\varphi)$  term should, of course, be replaced by a nonharmonic current-phase relation. However, in addition, the resistance and geometrical capacitance of SNS junctions (where  $R$  is a few ohms<sup>22</sup> and  $C$  is roughly  $10^{-16}$  fF) would correspond to  $Q \ll 1$ . In this so-called overdamped regime,<sup>23</sup> the expected  $I(V)$  dependence is  $V = \sqrt{I^2 - I_c^2}$ , and no sharp switching or hysteresis should be observed.<sup>20</sup> Experimentally, at low temperature, we find  $I_s/I_r$  between 3 and 7 (see Table I), and in other groups, hysteresis is always observed at low temperature [Dubos *et al.*<sup>12</sup> found 8 and Anthore found between 5 and 6 (Ref. 18)]. A similar discrepancy has already been pointed out in superconducting weak links by Song.<sup>24</sup> The large hysteresis was explained by the fact that the pair relaxation time in the weak link was no longer given by  $RC$  but by  $\hbar/\Delta$ . Following this analysis and as suggested by Ryazanov,<sup>25</sup> we replace the  $RC$  time by the diffusion time of the Andreev pairs in the normal region  $\tau_D = \hbar/E_{Th}$ . A comparison to the RSJ model is then achieved by replacing the capacitance with an effective capacitance  $C_{\text{eff}} = \tau_D/R$ . This yields  $I_c/I_r = \sqrt{2e/hR_N I_c} / \tau_D = \sqrt{2eR_N I_c} / E_{Th} = \sqrt{2b}$ . Table I shows that the measured ratio at low temperature is indeed of the order of this value.<sup>26</sup>

Note that heating of the sample once the SNS junction has switched to the resistive state will also cause hysteretic  $IV$  curves: The power injected in the normal wire may not be entirely dissipated by the substrate and superconducting contact phonons at low temperature, and heat conduction by the superconducting contacts is weak because of the superconducting gap. It is therefore probable that the electron temperature as the current is ramped down after switching is higher than before switching so that the experimental retrapping current may be smaller than the intrinsic retrapping current.

Since both heating and intrinsic charge relaxation depend on the wire length (although with different power laws), it is difficult at this stage to exactly determine the relative contribution of each effect to the hysteresis. However, the very shape of the  $IV$  curve is a clear indication that these SNS junctions are intrinsically hysteretic since a nonhysteretic (overdamped) junction would have a square-root dependence  $V = R\sqrt{I^2 - I_c^2}$  of the  $V(I)$  curve,<sup>20</sup> which is in contrast to the sharp jump observed at the transition in our junctions at low temperature. In addition, we find that the hysteresis amplitude only weakly depends on the flux through the squid: In the example of Fig. 6, going from constructive to destructive interference changes the switching current by a factor of 2, but the amplitude of the hysteresis  $I_s/I_r$  is reduced by roughly one-third. One would expect the hysteresis to be much more affected if it were caused by heating.<sup>27</sup>

Finally, measurements of the noise spectrum of long diffusive SNS junctions by Hoffmann *et al.*<sup>16</sup> suggest that the electron temperature is much less than 500 mK, even in the retrapping branch.

It is therefore safe to conclude that although electron heating may contribute to the hysteresis in the  $IV$  curve, intrinsic

TABLE II. Comparison between quantities determining the switching process for SIS and SNS junctions. Here,  $R_Q = h/e^2$  and  $b = eR_N I_c / E_{Th}$ .

	SIS	SNS
$eR_N I_c$	$\Delta$	$bE_{Th}$
$E_J$	$[\hbar/(2e)]I_c$	$[\hbar/(2e)]I_c = \frac{b}{4\pi} \frac{R_Q}{R} E_{Th}$
$\tau_R$	$RC$	$\hbar/E_{Th}$
$E_C$	$e^2/C$	$2\pi \frac{R}{R_Q} E_{Th}$
$\hbar\omega_p$	$\sqrt{\hbar 2e I_c / C}$	$\sqrt{2b} E_{Th}$
$Q$	$\omega_p RC$	$\sqrt{2b}$
$k_B T^*$	$\hbar\omega_p / (2\pi)$	$\frac{\sqrt{2b}}{2\pi} E_{Th}$

hysteresis is also present and most likely due to the relatively slow dynamics of the phase and charge in the long normal wire.

The inset of Fig. 5 shows that the hysteresis disappears at higher temperatures. This could be due to a lower  $I_c$  and to a more efficient heat dissipation at higher temperature, and therefore decreased heating. However, it may also be explained by the fact that the quality factor  $Q$  depends on temperature via the square-root dependence of the plasma frequency  $\omega_p$  upon  $I_c$  (see Table II). In the case of this sample Nb750, the switching current is divided by 8 between low temperature and 1 K, and the quality factor should thus lose a factor  $\sqrt{8} \approx 3$ , bringing the quality factor to 1 at 1 K, which corresponds to a strong damping and a nonhysteretic curve with square root  $V(I)$  dependence, as observed in Fig. 5.

### 3. Fluctuations of switching current

Since the escape is a stochastic process, the values of the switching current  $I_s$ , at which the junction switches from its superconducting to normal state, are characterized by a certain dispersion, which is related to the thermal activation or the quantum tunneling of the fictitious particle through the barrier. The dynamics of the SNS junction therefore also determines the probability distribution of the switching current.

We have measured the histograms of the switching current, following the technique used by Devoret *et al.*<sup>28</sup> The current is repeatedly swept (at a frequency of  $f=65$  Hz) from a small negative current to  $I_{\max} > I_c$ , and the current at which a finite voltage appears is recorded. Figure 7 shows a histogram of the switching current for a Nb/Au ring at  $\Phi/\Phi_0 = n + 1/2$ . The histograms of Al/Au junctions are similar. As expected from a switching phenomenon, the histogram is asymmetric, falling off more sharply at higher currents. The histogram is narrow, with  $\delta I_s / I_s$  roughly 1/1000.

Following the previous description of the hysteresis, in which the geometrical capacitance  $C$  is replaced by an effective one  $\tau_D/R$ , we can extrapolate the SIS theory to the SNS case. All the characteristic scales for SIS junctions and their correspondence for SNS junctions are listed in Table II.

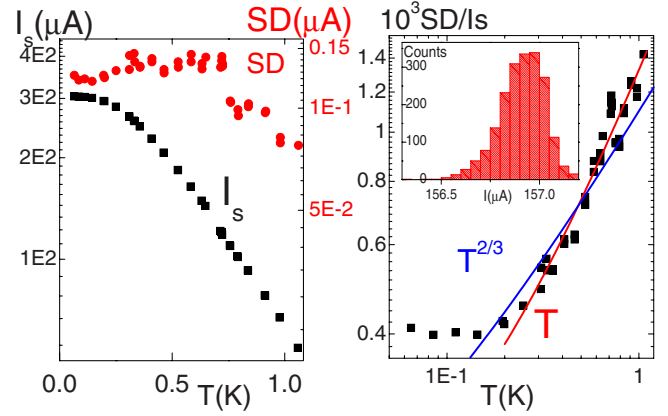


FIG. 7. (Color online) Left panel: Switching current  $I_s$  and width of the histogram [standard deviation (SD)] as a function of temperature for the short Nb dc squid (Nbsq750) at  $\Phi=0$ . Right panel: ratio of  $SD/I_s$ , compared to a linear and a  $T^{2/3}$  dependence. Fitting functions (continuous lines) are  $10^3 SD/I_s = 0.1 + T^{2/3}$  and  $10^3 SD/I_s = 1.18(T + T_0)$ , with  $T_0 = 128$  mK. Inset: Histogram of the switching current for  $\Phi/\Phi_0 = n + 1/2$  for the shortest junction Nb/Au ring at  $T = 60$  mK. The total number of counts is 2000.

Garg<sup>29</sup> calculated the width of the switching histogram of SIS junctions. This width depends on the damping and the origin of the escape rate (thermal or quantum). In the underdamped regime, which is our situation (see Table II), at high temperature, the particle should escape by thermal activation and the width is given by  $\delta I_s / I_s \approx (T/E_J)^{2/3}$ , but below a temperature  $T^* = \hbar\omega_p / 2\pi k_B$  of the order of  $E_{Th}$ , the particle escapes by quantum tunneling and the width of the histogram is expected to be  $\delta I_s / I_s \approx (E_{Th}/E_J)^{4/5}$ . Extrapolating these results to the SNS junction, the expected width is proportional to  $(T/E_J)^{2/3} = (R_N/R_Q \cdot T/E_{Th})^{2/3}$  in the thermally activated regime and proportional to  $(E_{Th}/E_J)^{4/5} = (R_N/R_Q)^{4/5}$  in the quantum regime. The predicted widths are therefore of the order of  $\delta I_s / I_s = 1/1000$ , as found experimentally at low temperatures. The  $2/3$  power law, however, in the thermally activated regime is not really found experimentally (see Fig. 7) in the shortest-junction Nb/Au ring.

## V. TEMPERATURE DEPENDENCE, THOULESS ENERGY, AND NORMAL STATE RESISTANCE

The critical current is predicted<sup>15,30</sup> to reach  $eR_N I_c(T=0) = 10.82 E_{Th}$  in the limit of infinitely long junctions ( $\Delta/E_{Th} = \infty$ ) and to be given by  $eR_N I_c(T=0) = b E_{Th}$ , with  $b$  smaller than 10.82 but within a few percent as soon as  $\Delta/E_{Th} > 10$ . The ratios  $b = eR_N I_s / E_{Th}$  at the lowest temperature (16 mK for Nbsq and Alsq samples, 60 mK for Alw samples) are listed in Table I and are within 50% of this value. The main uncertainty in calculating the ratio is in determining the normal state resistance. The Thouless energy  $E_{Th}$  is extracted with greater confidence from the temperature dependence of the switching current, as explained in the next paragraph.

The switching current can thus be defined (rather equivalently) as either the average or the most probable value out of a series of measurements and is plotted for 2000 measure-

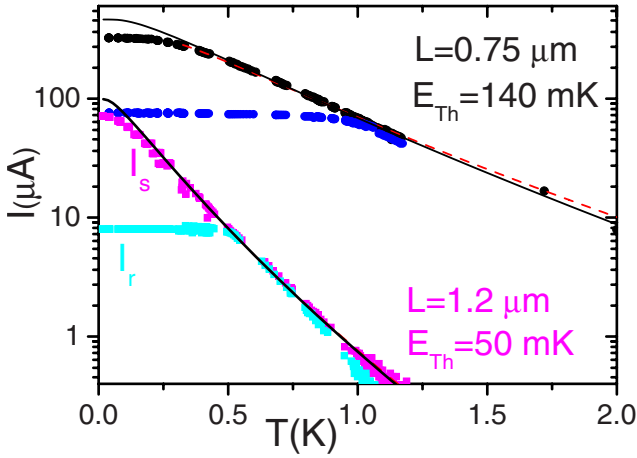


FIG. 8. (Color online) Switching and retrapping currents as functions of temperature for both Nb dc squids at the maximal switching current (comparison between experiment and theory). The filled dots and squares are the data points. The dashed lines are fits to the high temperature formula for the proximity effect [see Eq. (1) of Dubos *et al.* (Ref. 10), from which the Thouless energy is deduced]. The black lines are the numerical solutions to the Usadel equations using the Thouless energy deduced from the high temperature fit. The hysteresis disappears (i.e., the switching and retrapping currents are equal) at a temperature close to  $11E_{Th}$ .

ments as a function of temperature in Fig. 8. As is clear in Fig. 8, the decay of switching current above a few hundred millikelvins is roughly exponential: i.e.,  $I_s \approx e^{-T/\alpha E_{Th}}$ , with  $\alpha$  of order 9.<sup>30</sup> We used an approximate high temperature expansion [i.e., Eq. (1) of Dubos *et al.*,<sup>10</sup> which is valid when  $k_B T > 5E_{Th}$ ] to determine the Thouless energy and the normal state resistance (dashed lines). The full temperature dependence, which is obtained by a numerical integration of the Usadel equations using the determined Thouless energy, is also plotted as a continuous line in Fig. 8. For both Al and Nb samples, the high temperature decay of the switching current is well described by the Usadel calculation. At low temperatures, however, the predicted switching current is larger than that experimentally found (by roughly a factor of 2, for instance, 100  $\mu A$  instead of 70  $\mu A$  for the longest Nb dc squid (Nbsq1200) and 500  $\mu A$  instead of 250  $\mu A$  for the shortest dc squid (Nbsq750)]. The deviations from the theoretical prediction occur below 400 mK for the longest junction and below 200 mK for the shortest one. The switching current saturates at lower temperatures. We have no explanation for the deviations from theory at temperatures that are relatively high: Although the electronic temperature may be higher than the phonon temperature of the mixing chamber at the lowest temperatures (16–50 or 100 mK), it is improbable that the electron temperature be very different than the phonon temperature at temperatures higher than 100 mK.<sup>31</sup>

The fitting parameters  $R_N$  and  $E_{Th}$  are given in Table I, as well as the value of the ratio  $eR_N I_s / E_{Th}$ . The normal state resistance  $R_N$  extracted from the fit is somewhat (50%) smaller than that extracted from the  $dV/dI$  curves, and the  $eR_N I_s / E_{Th}$  product is also roughly 50% less than the maximum value of 10.82, which is expected at zero temperature

for an infinitely long normal wire and a perfect transparency.

The role of nonperfect transparency of the superconducting/normal (SN) interface was investigated in Ref. 32. Numerical integration of the Usadel equations shows that the main effect of a nontransparent interface is to renormalize the Thouless energy and to decrease the region of current saturation: Thus, an imperfect interface could not explain the slower variations with the temperature of the switching current at low temperature for the shortest Nb sample, as compared to the switching current variations: Whereas the switching current decays practically exponentially, the histogram width practically does not change with temperature at roughly 0.5% of  $I_s$ .

## VI. MAGNETIC FIELD DEPENDENCE

The variations of the switching current in a perpendicular magnetic field are central to our investigation. As for the conventional SIS dc squids, the SNS dc squid samples have a periodically oscillating switching current, whose period corresponds to a flux quantum  $\Phi_0 = h/2e$  through the loop area, as shown in Figs. 9–13. There are, however, features of the field dependence that have not been reported before, for instance, the absence of the Fraunhofer pattern in the decrease of switching current at larger field: The decay is monotonous and practically Gaussian with a field scale of one or several flux quanta through the normal wire.

### A. Modulation of the switching current by the magnetic field: The superconducting/normal/superconducting dc squid

First, we focus on the proximity dc squid interference patterns, as shown in Figs. 9 and 10, and compare them to the theory of a regular dc squid made of two tunnel SIS junctions in parallel.<sup>20</sup> The critical current  $I_c$ , which is the switching current in the absence of fluctuations, is given by

$$I_c^2 = (I_1 - I_2)^2 + 4I_1 I_2 \cos^2\left(\frac{\pi \Phi}{\Phi_0}\right) \quad (2)$$

$$= I_1^2 + I_2^2 + 2I_1 I_2 \cos\left(2\pi \frac{\Phi}{\Phi_0}\right), \quad (3)$$

with  $I_1$  and  $I_2$  as the critical currents of the two junctions and  $\Phi$  as the magnetic flux threading the squid loop. This critical current thus periodically oscillates with the field with a period of one flux quantum  $\Phi_0 = h/2e$  through the squid loop. The oscillation amplitude is maximum in symmetric squids and is reduced in squids whose junctions have different critical currents. The relative amplitude in noninductive squids is given by

$$r_{as} = \frac{I_c^{\max} - I_c^{\min}}{I_c^{\max}} = \frac{2 \min(I_1, I_2)}{I_1 + I_2}. \quad (4)$$

Such dc squid behavior is indeed demonstrated in our SNS dc squids, as shown in Figs. 9–13. Supercurrents of up to 330  $\mu A$  are modulated by 45%–88% (see Table I). The incomplete modulation, which corresponds to a ratio  $I_1/I_2$  between 1.3 and 3.4, can be attributed to slight differences in

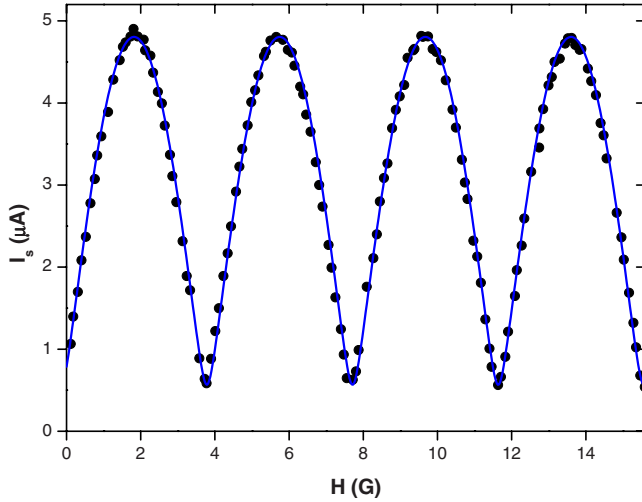


FIG. 9. (Color online) Switching current of Alsq1900 SNS dc squid as a function of the magnetic field at  $T=16$  mK (circles) and fit to Eq. (3) (line) showing the dc squidlike behavior. Here,  $I_1 = 2.1 \mu\text{A}$  and  $I_2 = 2.7 \mu\text{A}$ .

the geometry of the two normal wires to which the critical current is very sensitive. Indeed, the critical current of a long SNS junction scales as the inverse cube of the normal wire length.

The inductances  $L_1$  and  $L_2$  of the two branches of the squid also come into play in determining the shape of the modulation curve since they act to screen the external flux  $\Phi_{\text{ext}}$  by  $\delta\Phi = L_1 i_1 - L_2 i_2$ , where  $i_1$  and  $i_2$  are the currents through the two branches of the squid (and  $i_1 + i_2 = I$ ). In symmetric squids with  $L_1 = L_2$ , the screening induced is zero for fields corresponding to the maximum switching current since the flux induced by the screening current in one branch is exactly canceled by the flux induced by the same current in the other branch. The maximum effect of the screening flux produced by the inductance corresponds to half a flux quantum in the loop  $\Phi_{\text{ext}}/\Phi_0 \equiv 1/2 \pmod{1}$ . This explains the deviations from the simple cosine dependence seen in some samples (see, for instance, Fig. 10). In some cases, which correspond to  $L_1 \neq L_2$ , asymmetries with respect to reversals of the magnetic field or current are clearly visible (see Fig. 11). The switching currents  $I_s^{\text{up}}$  and  $I_s^{\text{dn}}$  measured on the positive and negative current branches of  $V(I)$  (while increasing the absolute value of the current in both cases) differ at a finite magnetic field by

$$\begin{aligned} I_s^{\text{up}}(-H) &\neq I_s^{\text{up}}(H), \\ I_s^{\text{dn}}(-H) &\neq I_s^{\text{dn}}(H). \end{aligned} \quad (5)$$

However, as expected from the global time reversal symmetry of the experiment,  $I_s^{\text{up}}(H) = -I_s^{\text{dn}}(-H)$ . These asymmetries have previously been calculated in Ref. 33 and measured in  $S/I/S$  dc squids.<sup>34</sup> They were also exploited by Clarke and Paterson<sup>9</sup> in larger area SNS dc squids: The authors controllably adjusted the asymmetry of the two superconducting branches and verified the corresponding asymmetry in the  $I_s(\Phi)$  curves. The current modulation in those

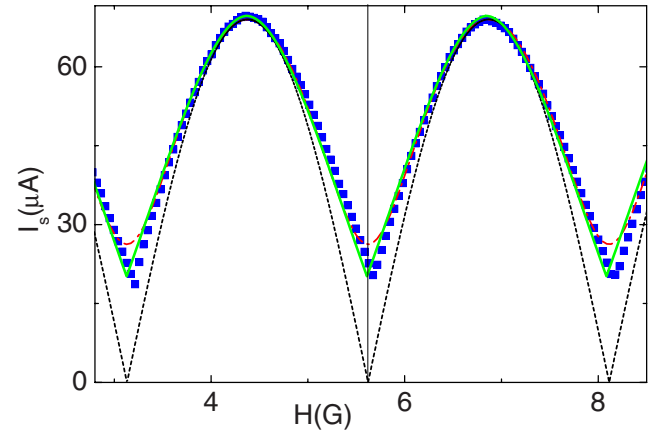


FIG. 10. (Color online) Dots: Switching current over three magnetic field periods for the longest Nb dc squid Nbsq1200, which is measured at 60 mK. The lines are the simulated curves corresponding to the same maximum switching current of  $70 \mu\text{A}$ : The black dotted curve corresponds to a noninductive squid with identical junctions (the same critical current), the red dashed-dotted curve corresponds to a noninductive squid with different junctions, and the green line corresponds to a squid with identical junctions but two inductive branches with identical inductance  $L=6$  pH.

SNS dc squids was less than 5%. As expected for self-inductance effects, the asymmetry and anharmonic distortion of the periodic oscillations are largest in samples with the largest critical current.

One also expects the intrinsic nonharmonicity of the current-phase relation of an SNS junction to cause a distortion in the switching current vs the field curve of an SNS dc squid: The amplitude of the  $m$ th harmonic in the  $\Phi_0$  periodic current phase relation is predicted<sup>15</sup> to vary like  $1/m^2$  and

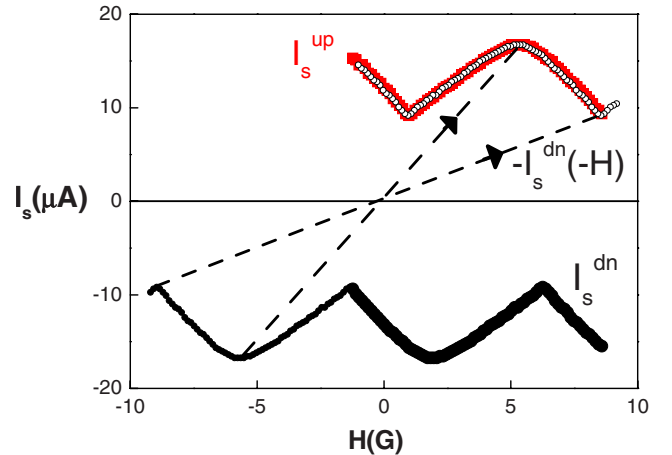


FIG. 11. (Color online) Sample Alsq900; comparison between the positive switching current in the up sweep (increasing current, red square symbols) and the negative switching current in the down sweep (decreasing current, black round symbols). The black curve with small open dots is the transformation of the down switching curve via the time reversal operation  $T[I_s^{\text{dn}}(H)] = -I_s^{\text{dn}}(-H)$  and is seen to be superimposed on  $I_s^{\text{up}}(H)$ , as expected from the global time-reversal symmetry of the experiment.

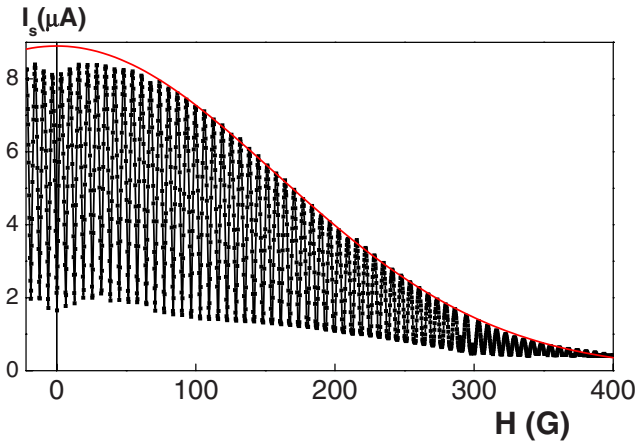


FIG. 12. (Color online) Switching the current as a function of the magnetic field for Al SNS dc squid Alsq1500 at 17 mK. The line is a Gaussian. A flux quantum through the normal wire corresponds to a field  $H_0=88$  G.

should therefore be detected at least up to the third order. However, it is straightforward to show that the critical current of an SNS dc squid with two symmetrical junctions is insensitive to even harmonics so that the harmonics content of the current-phase relation does not easily show up. To specifically test the anharmonicity of the current-phase relation in a long SNS junction, a strongly asymmetric setup with one reference SIS harmonic junction, such as the quantronium,<sup>35</sup> would, in principle, be more adequate. However, it would still be sensitive to self-inductance effects for large supercurrents.<sup>36</sup> Therefore, the best way to measure the various harmonics of the current phase relation of long metallic junctions is to directly measure the magnetic orbital response of a simple SNS ring, as was done recently using a magnetic Hall probe technique.<sup>37</sup>

### B. Decrease of the critical current at high field

We now discuss the decrease of the switching current on larger field scales. Experimentally, for the SNS dc squids, this large field scale behavior is extracted from the envelope of the oscillations, which in practice, are the maxima as a function of the field. In the following, we neglect the effect of the asymmetries in the squids and consider that the behavior in the field of these maxima is equivalent to the behavior in the field of a single SNS junction.

The first observation is that we do not observe the Fraunhofer diffraction pattern encountered in many experiments on wider and shorter SIS and SNS junctions.<sup>11,38,39</sup> Instead, we find a monotonous decay for all samples. In most cases, the decay is approximately Gaussian, with a field scale of one or a few flux quanta through the normal metal wire.

Qualitatively, in a semiclassical picture, the decay can be seen as due to dephasing induced by the magnetic field: Different diffusive Andreev paths in the normal metal acquire different phases. If the junction is wide, the phase along the NS boundary also varies, but in the limit of a normal wire much longer than it is wide, only the phase acquired during

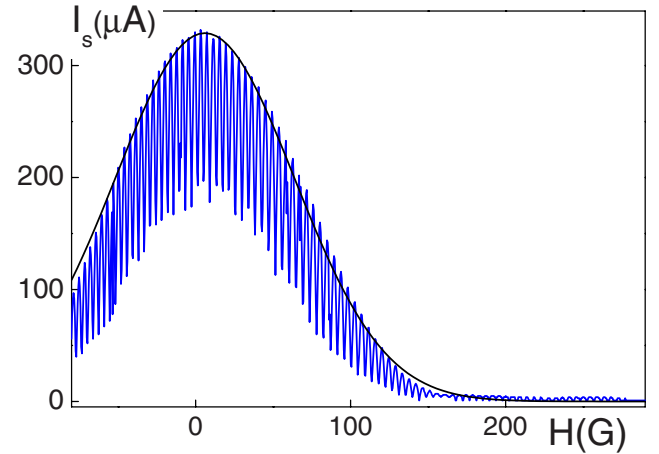


FIG. 13. (Color online) Switching the current of the short-junction Nb/Au dc squid Nbsq750 as a function of the magnetic field at 60 mK. The black line is a Gaussian. A flux quantum through the normal wire corresponds to a field  $H_0=66$  G.

the propagation across the normal metal is relevant.

Quantitatively, the average of the phase factor  $\phi(C) = \int_C \vec{A} d\vec{l} / \Phi_0$  acquired along a path  $C$  has been determined analytically in the one-dimensional (1D) limit (i.e., normal wire length  $L_N$ , which is much greater than width  $W$ ) using the solution of the field dependent diffusion equation.<sup>40</sup> This leads to

$$I_c(H) = I_c(0) \frac{\frac{\pi H}{\sqrt{3} H_0}}{\sinh \frac{\pi H}{\sqrt{3} H_0}}, \quad (6)$$

where  $H_0 = \Phi_0 / WL_N$  corresponds to a flux quantum through the normal part of the SNS junction [and  $\Phi_0 = h / (2e)$ ]. This calculation does not take into account the modification of the density of states in the normal wire. These experiments have also stimulated a full treatment of the proximity effect within the framework of the quasiclassical theory of superconductivity for diffusive systems.<sup>32</sup> In this approach, the description of the magnetic field dependence of the critical current for an arbitrary ratio between the wire length and its width requires, in general, solving the two-dimensional (2D) Usadel equations. However, in the 1D limit ( $L_N \gg W$ ), one can show that the magnetic field simply enters as a pair-breaking mechanism described by a depairing time  $\tau_H = 6\hbar^2 / (D_N e^2 W^2 H^2)$ . In this limit, the numerical results for the critical current for perfectly transmissive interfaces can be fit by a Gaussian function at low fields ( $H/H_0 < 3$ ),

$$I_c(H) = I_c(0) \exp - [a(H/H_0)^2]. \quad (7)$$

The coefficient  $a$  is worth 0.24 at zero temperature and decreases as  $T$  increases (see right panel of Fig. 15).

For low fields ( $H/H_0 < 2$ ), the semiclassical calculation [Eq. (6)] is also well approximated by a Gaussian, but the coefficient in the exponent is 0.55 instead of 0.24.

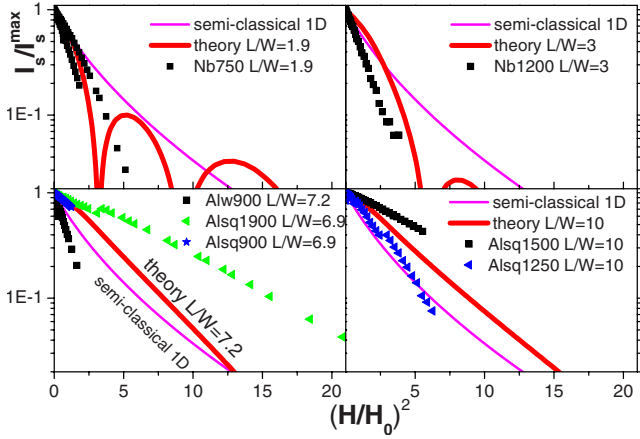


FIG. 14. (Color online) Field dependence of the normalized switching current for all samples at lowest temperatures and comparison with theory. For the samples with the squid geometry, the data points are the local maxima of the full (modulated) curves. The four panels correspond to four different aspect ratios of the normal wires. The continuous lines are the theoretical predictions of the Usadel equations at zero temperature for the exact aspect ratio of the junction. The prediction of the 1D semiclassical calculation [Eq. (6)] is the thin line. The vertical scale is logarithmic and the horizontal axis is the square of the magnetic field normalized by the field  $H_0$ , which corresponds to a flux quantum through the wire surface.

On the other hand, the numerical solution of the 2D Usadel equations shows that as the width increases, there is an onset of a magnetic interference pattern, i.e., the critical current does not monotonously decay with the field but it exhibits oscillations.<sup>32</sup> Finally, when the width becomes comparable to the length ( $W \sim L_N$ ), one recovers the well-known Fraunhofer pattern, where the critical current vanishes at multiples of  $\Phi_0$ .

The ratio  $L_N/W$  of our samples is, respectively, 2 and 3 for the short and long Nb samples and exceeds 7 for all Al samples (see Table I). To compare experiment and theory, we thus computed the predicted field dependence of the maximal switching current by using the Usadel equations with the experimental aspect ratio of the junctions. The calculated curves for both Nb SNS dc squids and two Al SNS samples are plotted in Fig. 14. It can be seen that the decay of the switching current is only qualitatively described by a theory. In particular, the theory predicts that the widest Nb/Au/Nb junction should exhibit relatively large oscillations of the maximum switching current with the field, which is not found in the experiment. It is also seen in the two lower panels that samples with identical aspect ratios can have very different field dependence scales.

Finally, we note that a similar monotonous decay of the switching current of an SNS wire was observed very recently in an applied parallel magnetic field and explained similarly by the depairing action of the magnetic field.<sup>41</sup>

One possible explanation for these discrepancies is the screening of the magnetic field by the superconducting contacts, as well as by the normal parts. Screening by the superconductor focuses the magnetic flux lines through the normal

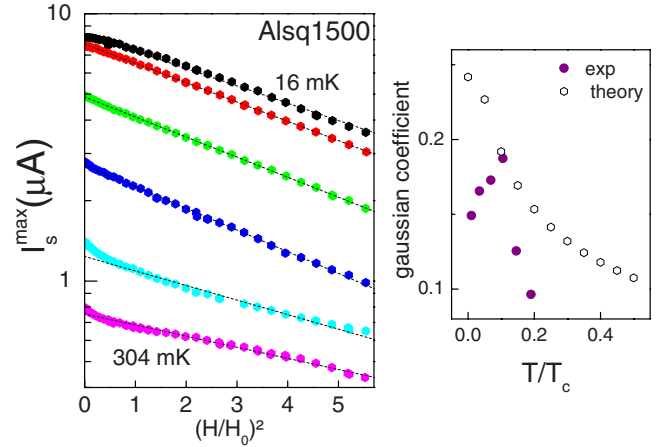


FIG. 15. (Color online) Field dependence of the switching current, as a function of temperature. Left panel: Maximum switching current (extracted from the modulated curves) as a function of the magnetic field for Al SNS dc squid Alsq1500, at temperatures of (from top to bottom) 16, 55, 110, 168, 233, and 304 mK (symbols). The vertical scale is logarithmic, and the horizontal axis is the square of the reduced magnetic field. The dashed lines correspond to a Gaussian decay. Right panel: Full symbols, temperature dependence of the coefficient of the Gaussian decay [coefficient  $a$  of Eq. (7)] extracted from the data, compared to the prediction of the Usadel equations (empty symbols).

metal, leading to a smaller  $H_0$ . On the other hand, screening by the normal metal tends to lead toward flux expulsion and a larger  $H_0$ . We have not yet included these effects in the calculations.

Figure 15 shows the field dependence of sample Alsq1500 at several temperatures, the temperature dependence of the Gaussian coefficient, and the comparison with the coefficients predicted by the Usadel equations. Here, experiment and theory also differ, which is a fact that may be due to the temperature dependence of screening of the magnetic field.

### C. Reentrant behavior at low field and low temperature

Certain samples exhibit a surprising increase of the switching current at low magnetic field (below 20 G, see Fig. 16) and at temperatures below 150 mK. A qualitatively similar effect but on a very different field scale was already observed on narrow superconducting wires made of MoGe and Ge (Ref. 42) and explained by the phase breaking of Cooper pairs induced by spin flip scattering on magnetic impurities.<sup>43,44</sup> Such spin flip scattering disappears when the magnetic moments are polarized under a magnetic field such that  $\mu_B B = k_B T$ . This would correspond to a field of a few hundred gauss in the present experiment, which is more than an order of magnitude larger than observed. Similar anomalies at low field were also reported by Xiong *et al.*<sup>45</sup> in narrow superconducting wires and attributed to phase fluctuations of the superconducting order parameter. Moreover, very recently,<sup>46</sup> such anomalies were found in only the thinnest superconducting Al wires (less than 20 nm wide). Other possible explanations include the following.

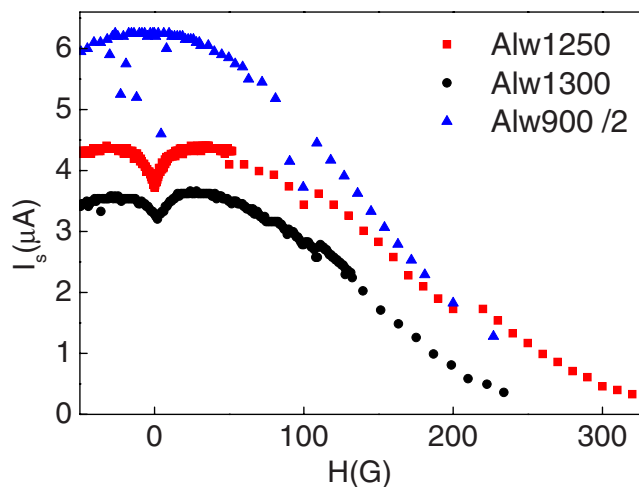


FIG. 16. (Color online) Switching current as a function of the magnetic field for the three Al/Au SNS wires at 17 mK. Switching the current of wire Alw900 has been divided by 2 for better comparison with the two other samples. Two of the three wires show a reentrant behavior.

(a) Quantum interference in the normal part of the junction. They are known to lead to weak localization corrections of the conductance in the absence of the proximity effect. The correction is of the order of  $e^2/h$ , which, for a wire of roughly  $1 \Omega^{-1}$ , corresponds to  $\frac{\delta I}{I} \approx 10^{-4}$ , i.e., much less than the 10% or 20% observed in the experiment. Moreover, the reentrance disappears above the temperature corresponding to the Thouless energy to which weak localization is not sensitive.

(b) Flux trapping in the superconducting wires during cooling of the samples. This can probably be excluded since no irreversibility or hysteresis is associated with this unusual field dependence.

(c) A last possibility could be a magnetic orbital effect in the form of quasiparticle persistent current loops, giving rise to strong paramagnetic orbital contributions similar to what

was observed in hybrid N/S cylinders at very low temperatures.<sup>47,48</sup>

It is noteworthy that this reentrance of  $I_s(H)$  is only present in the aluminum SNS junctions or squids, which have an abrupt interface between the normal and superconducting regions, and was never observed in the Nb junctions, in which the Au is also present under the Nb electrodes. It also occurs only in normal junctions whose length is between 1.2 and 1.5  $\mu\text{m}$  and was not detected in shorter or longer wires.

## VII. CONCLUSION

The SNS dc squid resembles its SIS counterpart, with a strong modulation of its switching current by the magnetic field, with a periodicity of one flux quantum in the loop. However, it also has unique features, such as a large switching current due to the low impedance of the normal metal. The  $IV$  curves and switching current histograms, because they depend on the intrinsic response functions of the normal metal wire, suggest the importance of investigating the dynamics of the Andreev states on time scales of the order of the diffusive time. In contrast to the SIS dc squid, the length and width of the normal part of the junctions can be varied at will. In the samples presented in this paper, the aspect ratio of the normal wires places them in the 1D or narrow 2D limit. We have shown that in this limit, the decay of switching current at high field does not show an oscillating interference pattern typical of wider junctions, but instead monotonously decays in a Gaussian-like manner. Finally, some samples have a surprising increase of switching current at low field, which is still not well understood.

## ACKNOWLEDGMENTS

We thank A. Anthore, M. Aprili, H. Courtois, R. Deblock, T. Heikkilä, F. Lefloch, I. Petkovic, H. Pothier, B. Reulet, V. Ryazanov, and B. Spivak for discussions and F. Pierre, D. Maily, and the LPN Laboratory for help with the Nb samples fabrication in their clean room facilities.

<sup>1</sup>A. Kasumov, M. Kociak, M. Ferrier, R. Deblock, S. Guéron, B. Reulet, I. Khodos, O. Stéphan, and H. Bouchiat, *Phys. Rev. B* **68**, 214521 (2003); A. Yu. Kasumov, K. Tsukagoshi, M. Kawamura, T. Kobayashi, Y. Aoyagi, K. Senba, T. Kodama, H. Nishikawa, I. Ikemoto, K. Kikuchi, V. T. Volkov, Yu. A. Kasumov, R. Deblock, S. Guéron, and H. Bouchiat, *ibid.* **72**, 033414 (2005); A. Yu. Kasumov, M. Kociak, S. Guéron, B. Reulet, V. T. Volkov, D. V. Klinov, and H. Bouchiat, *Science* **291**, 280 (2001); A. Yu. Kasumov, R. Deblock, M. Kociak, B. Reulet, H. Bouchiat, I. I. Khodos, Yu. B. Gorbatov, V. T. Volkov, C. Journet, and M. Burghard, *ibid.* **284**, 1508 (1999).

<sup>2</sup>E. Scheer, W. Belzig, Y. Naveh, M. H. Devoret, D. Esteve, and C. Urbina, *Phys. Rev. Lett.* **86**, 284 (2001).

<sup>3</sup>J.-P. Cleuziou, W. Wernsdorfer, V. Bouchiat, T. Ondarçuhu, and M. Monthieux, *Nat. Nanotechnol.* **1**, 53 (2006).

<sup>4</sup>J. A. van Dam, Y. V. Nazarov, E. P. A. M. Bakkers, S. De Franceschi, and L. P. Kouwenhoven, *Nature (London)* **442**, 667 (2006).

<sup>5</sup>I. O. Kulik and A. N. Omel'yanchuk, *Fiz. Nizk. Temp.* **4**, 296 (1978) [*Sov. J. Low Temp. Phys.* **4**, 142 (1978)].

<sup>6</sup>V. T. Petrashov, V. N. Antonov, P. Delsing, and T. Claeson, *Phys. Rev. Lett.* **74**, 5268 (1995); **70**, 347 (1993).

<sup>7</sup>H. Courtois, Ph. Gandit, D. Maily, and B. Pannetier, *Phys. Rev. Lett.* **76**, 130 (1996).

<sup>8</sup>Controllable SNS dc squids, with an adjustable nonequilibrium population in the N wire, were fabricated and described in J. J. A. Baselmans, A. F. Morpurgo, B. J. van Wees, and T. M. Klapwijk, *Nature (London)* **397**, 43 (1999); J. J. A. Baselmans, T. T. Heikkilä, B. J. van Wees, and T. M. Klapwijk, *Phys. Rev. Lett.* **89**, 207002 (2002); J. J. A. Baselmans, B. J. van Wees, and T.

- M. Klapwijk, Phys. Rev. B **65**, 224513 (2002); Appl. Phys. Lett. **79**, 2940 (2001).
- <sup>9</sup>Large SNS junctions in a dc squid configuration were in fact measured by John Clarke and James L. Paterson, Appl. Phys. Lett. **19**, 469 (1971); But these SNS dc squids were purposely very inductive. See also J. Clarke, Proc. R. Soc. London, Ser. A **308**, 447 (1969); Phys. Rev. B **4**, 2963 (1971).
- <sup>10</sup>P. Dubos, H. Courtois, B. Pannetier, F. K. Wilhelm, A. D. Zaikin, and G. Schön, Phys. Rev. B **63**, 064502 (2001); P. Dubos, H. Courtois, O. Buisson, and B. Pannetier, Phys. Rev. Lett. **87**, 206801 (2001).
- <sup>11</sup>H. B. Heersche, P. Jarillo-Herrero, J. B. Oostinga, L. M. K. Vandersypen, and A. F. Morpurgo, Nature (London) **446**, 56 (2007).
- <sup>12</sup>J. P. Heida, B. J. van Wees, T. M. Klapwijk, and G. Borghs, Phys. Rev. B **57**, R5618 (1998).
- <sup>13</sup>J. Kutchinsky, Ph.D. thesis, Technical University Denmark, 2001.
- <sup>14</sup>P. Billangeon and R. Deblock (private communication).
- <sup>15</sup>T. T. Heikkilä, J. Särkkä, and F. K. Wilhelm, Phys. Rev. B **66**, 184513 (2002).
- <sup>16</sup>C. Hoffmann, F. Lefloch, M. Sanquer, and B. Pannetier, Phys. Rev. B **70**, 180503(R) (2004); C. Hoffmann, Ph.D. thesis, Université Joseph Fourier, Grenoble, 2003.
- <sup>17</sup>P. Joyez, D. Vion, M. Götz, M. Devoret, and D. Esteve, J. Supercomput. **12**, 757 (1999).
- <sup>18</sup>A. Anthore (private communication).
- <sup>19</sup>Nathan Argaman, arXiv:cond-mat/9709001 (unpublished).
- <sup>20</sup>M. Tinkham, *Introduction to Superconductivity*, 2nd ed. (McGraw-Hill, New York, 1996).
- <sup>21</sup>A. T. Johnson, C. J. Lobb, and M. Tinkham, Phys. Rev. Lett. **65**, 1263 (1990).
- <sup>22</sup>The resistance that should enter here is the quasiparticle resistance at frequency  $\omega_p$ . At this frequency, which is of the order of the minigap induced in the metal, the quasiparticle energy is sufficient to overcome the minigap, and thus  $R_{qp} \approx R_N$ .
- <sup>23</sup>M. T. Levinsen, Rev. Phys. Appl. **9**, 135 (1974).
- <sup>24</sup>Y. Song, J. Appl. Phys. **47**, 2651 (1976).
- <sup>25</sup>V. V. Ryazanov (private communication).
- <sup>26</sup>Of course Andreev pairs can be coherent for a longer time than the diffusion time  $\tau_D$ . This fact gives rise for instance to the nonharmonic current phase relation, where the  $n$ th harmonic is associated with a time  $n\tau_D$ . Therefore, it is probable that a multiplicative factor should be included in front of  $\tau_D$ , although an exact theory is lacking.
- <sup>27</sup>A. T. Johnson, C. J. Lobb, and M. Tinkham, Phys. Rev. Lett. **65**, 1263 (1990).
- <sup>28</sup>M. H. Devoret, Daniel Esteve, John M. Martinis, Andrew Cleland, and John Clarke, Phys. Rev. B **36**, 58 (1987).
- <sup>29</sup>Anuparm Garg, Phys. Rev. B **51**, 15592 (1995).
- <sup>30</sup>F. K. Wilhelm, A. D. Zaikin, and G. Schön, J. Low Temp. Phys. **106**, 305 (1997).
- <sup>31</sup>Other experiments conducted on mesoscopic samples with the same apparatus (same dilution refrigerator, same filtering), clearly saw temperature dependences down to 30 or 50 mK. However none of those samples consisted of normal wires connected to small superconducting contacts, for which heat conduction is small).
- <sup>32</sup>J. C. Hammer, J. C. Cuevas, F. S. Bergeret, and W. Belzig, Phys. Rev. B **76**, 064514 (2007); J. C. Cuevas and F. S. Bergeret, Phys. Rev. Lett. **99**, 217002 (2007).
- <sup>33</sup>A. Barone and G. Paterno, *Physics and Application of Physics and Applications of the Josephson Effect* (Wiley, New York, 1982), Chap. 12.
- <sup>34</sup>F. Balestro, Ph.D. thesis, Université Joseph Fourier, Grenoble, 2003.
- <sup>35</sup>B. Huard, Ph.D. thesis, Université Paris 6, 2006.
- <sup>36</sup>A. Martín-Rodero, A. Levy Yeyati, and F. J. García-Vidal, Phys. Rev. B **53**, R8891 (1996).
- <sup>37</sup>M. Fuechsle, J. Bentner, D. A. Ryndyk, M. Reinwald, W. Wegscheider, and C. Strunk, arXiv:0707.4512 (unpublished).
- <sup>38</sup>R. C. Jaklevic, J. Lambe, J. E. Mercereau, and A. H. Silver, Phys. Rev. **140**, A1628 (1965).
- <sup>39</sup>S. Nagata, H. C. Yang, and D. K. Finnemore, Phys. Rev. B **25**, 6012 (1982); H. C. Yang and D. K. Finnemore, *ibid.* **30**, 1260 (1984); S. L. Miller and D. K. Finnemore, *ibid.* **30**, 2548 (1984).
- <sup>40</sup>G. Montambaux, arXiv:0707.0411 (unpublished).
- <sup>41</sup>M.S. Crosser, Jian Huang, F. Pierre, Pauli Virtanen, Tero T. Heikkilä, F. K. Wilhelm, and Norman O. Birge, Phys. Rev. B **77**, 014528 (2008).
- <sup>42</sup>A. Rogachev, T.-C. Wei, D. Pekker, A. T. Bollinger, P. M. Goldbart, and A. Bezryadin, Phys. Rev. Lett. **97**, 137001 (2006).
- <sup>43</sup>V. Barzykin and A. Zagorskii, Superlattices Microstruct. **25**, 797 (1999).
- <sup>44</sup>K. D. Usadel, Phys. Rev. Lett. **25**, 507 (1970).
- <sup>45</sup>P. Xiong, A. V. Herzog, and R. C. Dynes, Phys. Rev. Lett. **78**, 927 (1997).
- <sup>46</sup>M. Zgirski, K. P. Riikonen, V. Touboltsev, and K. Yu. Arutyunov, Phys. Rev. B **77**, 054508 (2008).
- <sup>47</sup>F. B. Müller-Allinger and A. C. Mota, Phys. Rev. Lett. **84**, 3161 (2000).
- <sup>48</sup>Christoph Bruder and Yoseph Imry, Phys. Rev. Lett. **80**, 5782 (1998).